

CENTRIFUGE MODELING OF FAULT RUPTURE PROPAGATION THROUGH A DRY SAND

○Jea Woo LEE¹, Go TABUCHI², Kazuhito SUZUKI² and Masanori HAMADA³

¹ Ph.D. Candidate, School of Science and Engineering, Waseda University
Tokyo, 169-8555, Japan, jay-lee@aoni.waseda.jp

² Graduate Student, School of Science and Engineering, Waseda University
Tokyo, 169-8555, Japan, kazuhito@moegi.waseda.jp

³ Professor, School of Science and Engineering, Waseda University
Tokyo, 169-8555, Japan, hamada@waseda.jp

著者らは、地下断層の変位による砂質地盤中の破壊の伝播を実験的および解析的手法を用いて検討している。重力場および遠心載荷場での逆断層の模型実験において、地盤の破壊型、地表面における破壊の出現位置、地表面の形状は、地下断層の傾斜角および地盤密度の影響を顕著に受けることが確認された。さらに、砂質地盤での模型実験では、拘束圧が破壊の伝播に影響を及ぼしていることも確認された。

Key Words : fault rupture propagation, earthquake surface fault, fault box test, centrifuge test

1. INTRODUCTION

Recent huge earthquakes have revealed that earthquake fault ruptures on ground surface could cause severe damages to the major infrastructures located within the zone of faulting. Even though surface fault rupture is not a new issue, there is no construction code in Japan containing any type provisions for reducing the risks yet. This may be owing to the infrequent occurrence of fault surface ruptures and also the difficult task of estimating the related permanent deformations due to many unknown factors such as possible fault location, geometry and motion; and mechanical properties of the soil deposit. Nevertheless, a few of studies on this subject using physical model have been continuously performed for past more than twenty years in Japan and US. Cole et al. (1984) presented a theoretical model to predict the location of surface rupture based on the results from a series of 1-g fault box tests of alluvial sand. Bray et al. (1994) released the experimental and analytical results of studies on the response of saturated clay soils to bed rock displacement. Several series of fault box tests under 1-g condition using Toyoura sand and silica sand in dry were carried out to investigate the effect of fault type on the required displacement to form shear rupture by Tani et al. (1994, 1999). These studies mostly have been carried out with concern only about the pattern of rupture propagation and the location of surface rupture. However, as shown in

Fig. 1, the rupture propagation can accompany the distortion of ground surface depending upon the ductility of the material overlying the active fault. Hence, it is also in need to figure out how much the

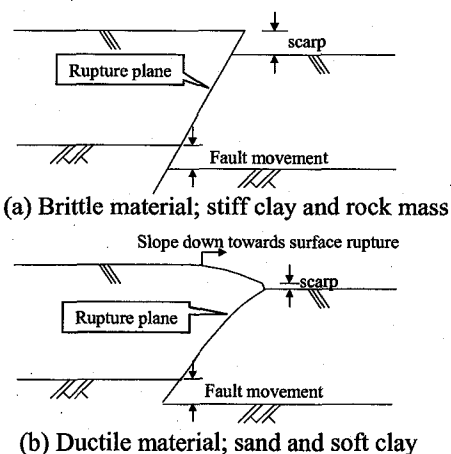


Fig. 1 Earthquake fault rupture due to reverse fault

extent of distortion of surface ground appears according to the differential displacements at bedrock fault.

Moreover, most of experimental studies seem to be conducted under low level of confining stresses, which may yield somewhat different trends from the actual behavior considering the thickness of deformable soil layers in real field.

In this study a series of physical model test under both of 1-g and centrifuge conditions has been

carried out to examine the rupture propagation in dry sand with particular concern on dip-slip fault. The effects of inclination of fault plane and fault types have been examined through the 1-g fault tests with two different densities. The rupture patterns induced by fault movements for reverse fault have been also investigated through comparison among the results from the tests under various gravitational conditions. The investigation into rupture patterns under various gravitational conditions shows that the prediction of location of the surface rupture in a sandy soil mass using a physical model under 1-g condition can be largely affected by the thickness of model itself and the results from which should be meaningfully verified with those from centrifuge tests

2. OUTLINE OF PHYSICAL MODELS FOR FAULT RUPTURE PROPAGATION

(1) Preparation of Testing Apparatus

Two kinds of testing devices have been introduced to conduct the dip-slip faulting tests under single gravity and centrifuge condition in this study. The device for single gravity test, Apparatus I, see Fig. 2 (a), was built up with steel frame and glass-walled box of which in-plane dimension is 2.0m-0.5m-1.0m in length, width and depth. The adjustable rolling hopper was assembled to place the dry sand in the testing box at a uniform density. On the other hand, the testing apparatus for centrifuge tests, Apparatus II, was constructed with a steel frame consisted of 30mm thick steel plates and an acrylic board with thickness of 50mm on one side of the box. The dimension of the in-plane apparatus is 1.2m-0.8m-0.45m in length, width and depth. One-third of the testing box could be moved up along a fixed dip angle - 45° in this study - to relative to the fixed part using double 200tonf-capacity hydraulic jacks. To minimize the influence of wall friction, Teflon sheet was attached on each inner side of wall before starting to put sand into the box.

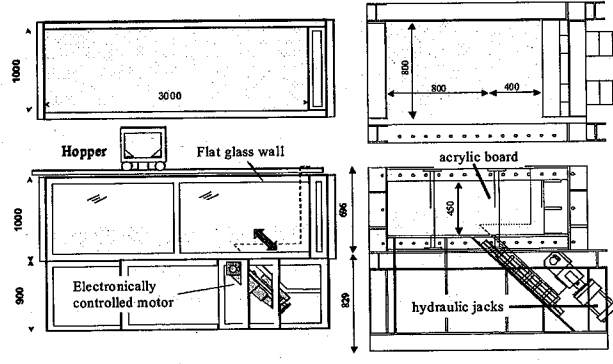


Fig. 2 Setup of testing apparatus used in fault tests (in mm)

(2) Testing Procedure

The procedure for each fault test in this study is summarized as bellow;

- i) Preparation of uniform sand layer using hopper with installation of black sand grid and target,
- ii) Activation of up/down movement of deck to the every incremental displacement with constant speed of 2mm/min.,
- iii) Taking photos of both sides of deformed specimen and surface of soil mass at every increment of vertical displacement,
- iv) Repetition of processes described as ii) and iii) to required offset to form complete shear ruptures to surface of model.

(3) Specimen for Test

The silica No. 7 was commonly used in both of the 1-g tests and the centrifuge tests. As for the 1g-tests, the effect of soil density was considered but for the centrifuge tests only dense sand was included as the specimen for the tests. The parameters related to soil deposit are summarized in Table 1.

TABLE 1: SOIL PARAMETERS USED IN TESTS

Material Type	Silica Sand No. 7
Average Grain size (D_{50})	0.157mm
Uniformity Coeff. (U_c)	1.55
Coeff. of Curvature (U_c')	0.946
Relative Density (D_r)	Loose : $59 \pm 4\%$ (1-g) Dense : $83 \pm 4\%$ (1-g), $74 \pm 6.58\%$ (centrifuge)
Dry density (γ)	$1.401 \text{tonf/m}^3 \leq \gamma \leq 1.452 \text{tonf/m}^3$

(4) Testing Cases

The testing cases performed under 1-g and centrifuge condition is summarized in Table 2

TABLE 2: Testing Cases for 1-g and centrifuge fault box tests

Type of Fault	1-g test		Centrifuge test
	Reverse fault	Normal fault	
Dip angle of fault (θ)	$30^\circ, 45^\circ, 60^\circ$ ($H=20 \text{ cm}$)	$30^\circ, 45^\circ, 60^\circ$ ($H=20 \text{ cm}$)	45° only
Thickness of ground model (H)	10 cm, 15 cm, 20 cm, 25 cm, 30 cm, 40 cm, 60 cm	20 cm	$20 \text{ cm} \times 20G = 4.0 \text{m}$ $20 \text{ cm} \times 30G = 6.0 \text{m}$ $15 \text{ cm} \times 50G = 7.5 \text{m}$ $30 \text{ cm} \times 30G = 9.0 \text{m}$

3. OBSERVED BEHAVIOR FROM TESTS

(1) Rupture patterns from fault box tests

The typical pattern of propagation of fault rupture through a sandy soil deposit can be obviously seen in the photographs shown in Fig. 3. Reverse fault

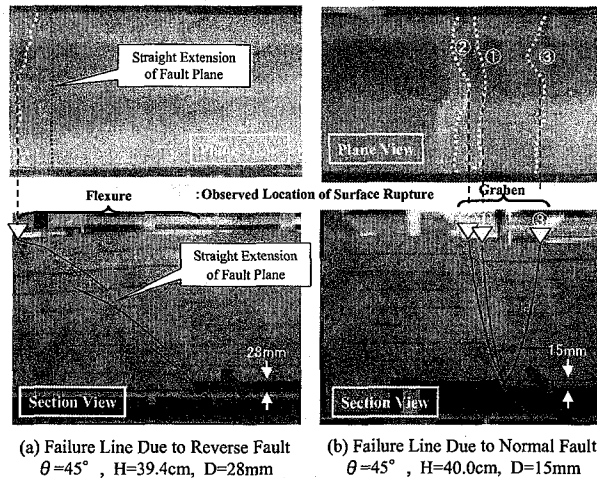


Fig. 3 Section and plan view of fault ruptures in reverse/normal faulting test with dip angle=45°

tended to gradually decrease in dip near the surface of ground and finally reached to the ground surface farer than the extension of fault plane with respect to the distance from the bedrock fault. Most of fault ruptures with reverse fault appeared the plural number of failure planes as shown in Fig. 3 (a). Particularly the larger the thickness of ground model was, the more the number of failure planes developed. In addition, as for reverse fault, the differential displacement at the bedrock fault tended to propagate to the ground surface spreading out over a wide zone rather than proceeding upward along a straight line which might be expected to come into view at ultimately brittle material. Accordingly this formed the distortion of surface ground that is called "flexure" as shown in Fig. 3 (a). On the contrary, normal faults were seen to produce rather distinct failure planes, all of which increased in dip as they approached the ground surface. For normal fault the differential displacement at bedrock tended to create a group of three singular failure planes, each of which took place sequentially as shown in Fig. 3 (b). The failure planes numbered by ① and ② in Fig. 3 (b) first took place at early stage of normal fault and a refraction on the soil-bedrock contact with subsequent fault movement produced the third failure plane numbered by ③. These successively developed failure planes formed a subsided area surrounded by the second and third failure planes, which is called "graben". Besides, the shapes of fault rupture appeared in the centrifuge models are illustrated in Fig. 4. These features also exhibited the same nature

with those in 1-g tests by showing the decrease in dip near the ground surface. However, comparing between the results from the 1-g tests and the centrifuge tests, the rather unique rupture surface with somewhat thicker failure surfaces than those of 1-g tests could be founded in case of the centrifuge tests whereas the rupture surfaces from 1-g tests appeared to frequently form plural numbers of failure lines with increase of the thickness of model.

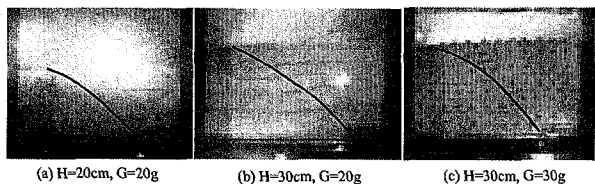
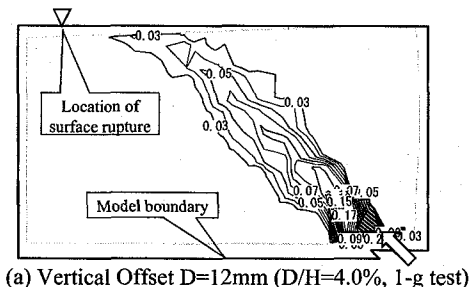


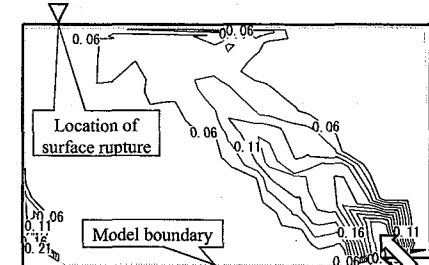
Fig. 4 Selected photos corresponding to three models in fault test on dense sand under centrifuge condition

(2) Shear strain distribution in soil mass

To figure out the development of maximum shearing strains in soil mass during fault rupture propagation, the contours of maximum shear strain in the model were calculated using the measured displacement vector during an experiment. As shown in the Fig. 5, the calculated contours of maximum shear strains corresponding to 4.0% of the normalized vertical offset show that the region of concentrated shear strains developed extending to the free surface of ground model as the observed failure surface during the test reached the model surface. At the same time, the value of maximum shear strain contour that appeared to approximately coincide with the observed failure surface was analyzed as ranging 0.03~0.04 for dense sand in 1-g tests and 0.05~0.06 for centrifuge tests.



(a) Vertical Offset D=12mm (D/H=4.0%, 1-g test)



(b) Vertical Offset D=19mm (D/H=6.5%, centrifuge test)

Fig. 5 Acquisition of maximum shear strain contour

4. DISCUSSIONS

(1) Location of Surface Fault Rupture

Based on the rupture patterns observed from the testing results, the key sketch for examination of rupture pattern is depicted as Fig 6.

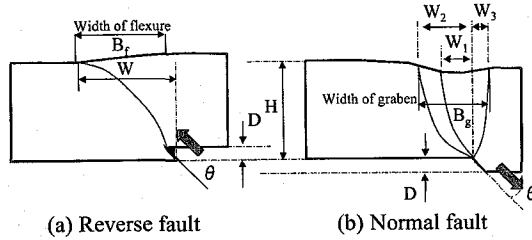


Fig. 6 Model for the evaluation of rupture patterns

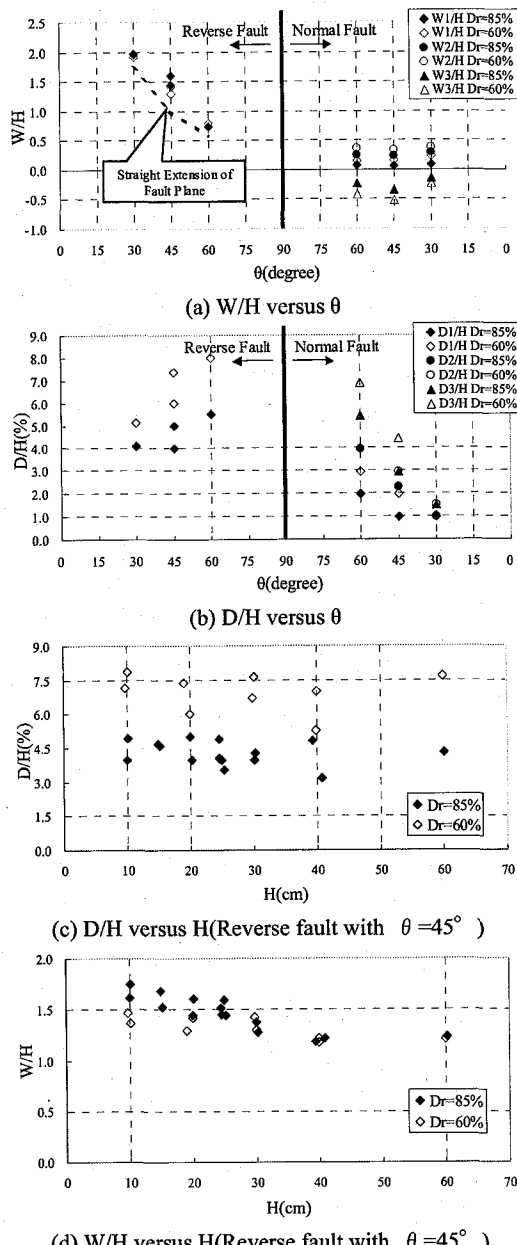


Fig. 7 Variation of W/H and D/H as a function of θ and a function of H from 1g test

Fig. 7 shows the relationship between the location of surface rupture and its relating factors from 1-g tests. As shown in Fig. 7 (a) and (b), as for the reverse faults, there appeared a definite inclination of the value of W/H to down with increase of the dip angle whereas there was only a little change in value for the normal faults. However, it appeared to be a reverse tendency in the variation of D/H . Besides, it can be seen in Fig. 7 (c) that the required vertical offset to form a complete fault rupture in sand mass mainly depends on the density of soil itself but appears to be independent of the thickness of model. Fig. 7 (d) indicates from the 1-g fault tests that the distance W is apparently associated with the thickness of model and coming closer to the point the fault intersects with increase of the height of soil mass. This implies that the rupture pattern could change as the thickness of the soil mass is varied under low confining pressure.

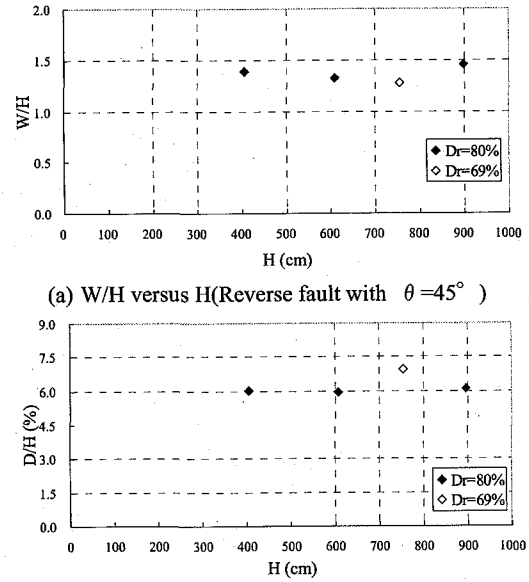


Fig. 8 W/H, D/H versus model thickness from centrifuge

In the meantime, Fig. 8 shows the relationship between the location of surface rupture and the model thickness from the centrifuge tests. It can be noticed from Fig. 8 (a) the figure that the values of W/H appeared to range between 1.2~1.4 without showing no definite tendency relating to the variation of model thickness, which is showing somewhat different tendency in the 1-g tests. And it can be also seen from Fig. 8 (b) that the ratios of D/H are also independent of the model thickness, which is the same trend as those in 1-g models.

(3) Width of Distorted Surface Regarding Dip Angle and Model Thickness

① Width of flexure and graben vs Dip Angle

Fig. 9 shows that the widths of flexure resulted from reverse faults were observed to vary depending upon the dip angle, and the fault movement with relatively low dip angle tends to produce the large width of flexure. Besides, the widths of graben from normal faults appeared to be not so much depending on the dip angle as the flexures did. But the soil density gave a remarkable difference regarding the width of flexure and graben that the looser sand tended to produce larger widths of flexure and graben than the denser sand when the fault rupture reached to the ground surface.

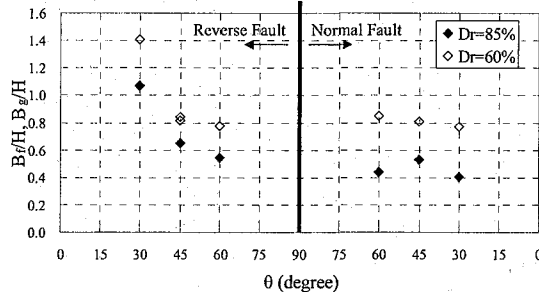


Fig. 9 Bf/Bg versus dip angle

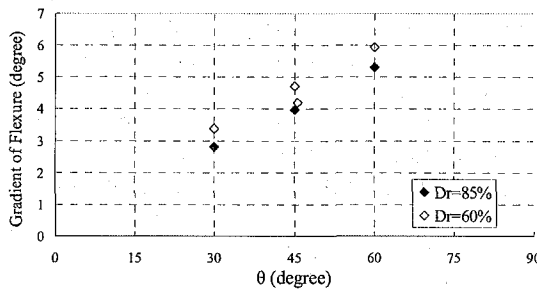


Fig. 10 Gradient of flexure versus dip angle

On the other hand, the gradient of flexure become smaller as the dip angle is decreased for reverse fault as shown in **Fig. 10**. This infers that the reverse faults with a shallow dip angle tend to spread out more widely than those with a deep dip angle as the rupture plane propagates up through the ground model. Accordingly it can be said that the denser sand underwent the reverse fault with a deep dip angle may cause more severe distortions of the ground surface that is so damaging to the structures nearby.

② Width of flexure vs Model Thickness

The widths of flexure have been investigated by changing the thickness of model for the reverse fault with a fixed dip angle of 45 degree. It appears from **Fig. 11** that the ratio of width of flexure to model thickness was uniform with respect to the change of model thickness. Moreover, this tendency also came in sight at the investigation about the gradient of flexure regarding the change of model thickness as plotted in **Fig. 12**. This implies that the ground deformation rupture induced by fault movements at the specific displacement at bedrock that can bring

about a surface fault rupture may be affected mainly by the dip angle and the ductility of soil rather than the model thickness.

And this trend can be confirmed at the results from centrifuge models as shown in **Fig. 13**.

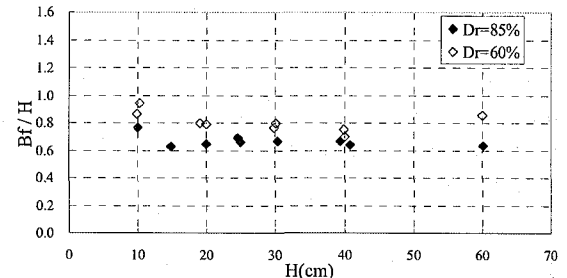


Fig.11 Width of flexure versus model thickness

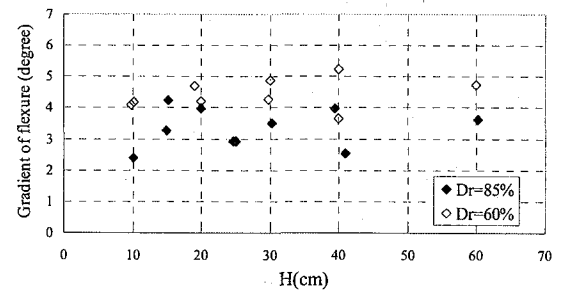


Fig.12 Gradient of flexure versus model thickness

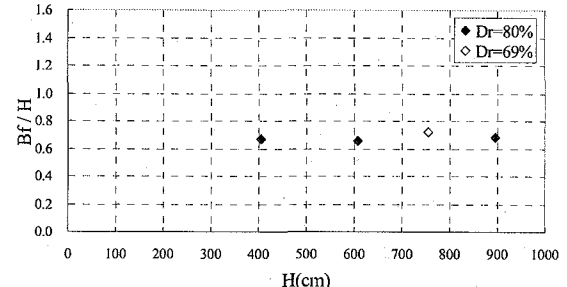


Fig.13 Width of flexure versus model thickness

(3) Effect of confining pressure on rupture

As mentioned previously, two series of reverse fault tests at 1-g and centrifuge conditions in this study provided us an observable finding presenting the change in the location of surface fault in accordance with confining stresses, which means the patterns of rupture propagation vary depending upon the stress levels.

This stress dependent characteristic of fault rupture propagation can be understood by taking the dilatant behavior of granular soil into consideration. Similar to Stone et al(1992)'s achievement, the author's experiments in 1-g condition exhibited an abrupt transformation of localized shearing deformation within a granular soil mass that was owing to the change of the dilation angle for the soil during process of shearing deformation as illustrated in **Fig. 14**. This implies that relatively large bedrock displacement in thicker models required to rupture the model surface caused greater change of the

dilation angle during the course of tests so that the initial surface failure could encounter kinematic incompatibility and might create a new localized shear region noted as ②~④ failure planes in Fig. 14. Hence, provided that a significant value of dilation angle and its decrease to zero during shearing process for a isotropic dry sand at low confining pressure are validly expected, it can be understood reasonably that the shear zone patterns in the soil change with a definite tendency at the stress levels in which the 1-g tests were implemented.

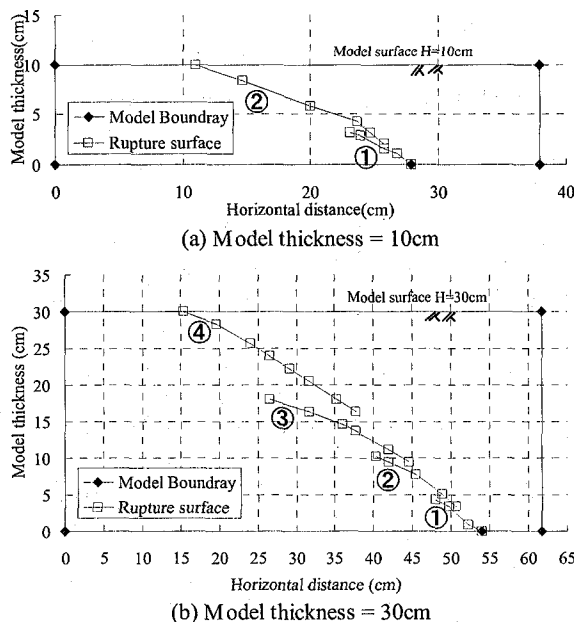


Fig. 14 Multiple failure surfaces observed in 1-g models

On the contrary, as shown in Fig 15, there appeared the identical pattern of rupture propagation without any obvious transformation of localized shearing region for the centrifuge models. This result indicates that the volume change tendency of the sand under centrifuge condition little varies owing to the increase of confining pressure. Moreover, the dilation angle of the sand itself will be lessened according to increasing the stress level.

In brief, this character of granular soil may be able to make the singular rupture pattern regardless of change of model thickness under high confining

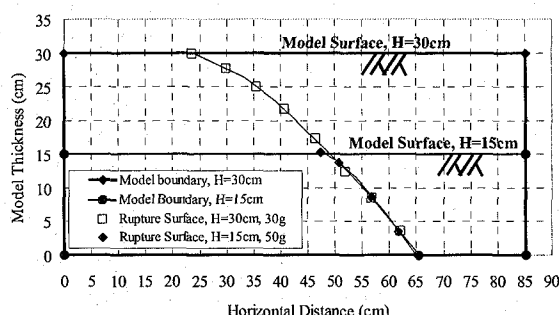


Fig. 15 Identical rupture patterns in centrifuge models

pressure, whereas it causes the individual rupture pattern as to model thickness under extremely low confining pressure, so that the location of surface rupture may change depending upon the different rupture pattern regarding model thickness.

5. CONCLUSION AND FUTURE STUDIES

The location of surface rupture and the width of flexure and graben responding to the affecting factors such as the type of faults, the density of soil and the dip angle of fault plane were evaluated from 1-g and centrifuge fault box tests. It is founded that changing the angle of fault plane with reverse fault could greatly affect the location of surface fault rupture. And the results from 1-g model tests with change of its thickness indicate that the location of surface rupture might be definitely influenced by model thickness at low confining pressure. By comparison with the results from centrifuge models, it is confirmed from this study that the physical models at 1-g condition for fault rupture propagation might provide a properly simulating method to approximately understand the response of sandy soil over the various types of bedrock fault movement.

However, for further understanding of the phenomenon to consider a mitigation method against hazards in real fields, an adequate centrifuge model should be taken into reproduction of fault rupture propagation to predict that behavior as close to real phenomenon as possible.

ACKNOWLEDGMENTS : The authors wish to thank the great dedication of Dr. T. Matsuda and his staffs in Dynamics Research Center of Obayashi Cooperation, Tokyo, Japan to the centrifugal model tests on this subject.

REFERENCES

- 1) Bray, J. D., Seed, R. B., and Seed, H. B., Analysis of earthquake fault rupture propagation through cohesive soil, *Journal of Geotech. Engrg.*, ASCE, Vol. 120, No 3, pp. 562-580, 1994
- 2) Cole, D. A., Jr., and Lade, P. V., Influence zones in alluvium over dip-slip faults. *Journal of Geotech. Engrg.*, ASCE, Vol. 110, No. GT5, pp. 599-615, 1984
- 3) Cundall, P. and Board, M., A microcomputer program for modeling large-strain plasticity problems, *Numerical Methods in Geomechanics*(Innsbruck 1988), Balkema, pp. 2101~2108, 1988
- 4) Johansson, J. and Konagai, K., Fault surface rupture experiments: a comparison of dry and saturated soils, *Proceeding of 27th Symposium on Earthquake Engineering*, JSCE, 2004.
- 5) Stone, K. J. L. and Wood, D.M., Effects of dilatancy and particle size observed in model tests on sand, *Soils and Foundations*, JSSMFE, Vol. 32, No 4, pp. 43-57, 1992
- 6) Tani, K., Ueta, K. and Onizuka, N., Scale effect of quaternary ground deformation observed in model tests of vertical fault, *Proc. of 29th Japan National Conference on SMFE*, pp. 1359~1362, 1994